I. Introduction

1.1 General Purpose

The purpose of this thesis is to present two multiscale analyses of inland tropical cyclone (TC)–midlatitude jet interactions. More specifically, the main focus will be to document the synoptic-scale environment and underlying mesoscale processes responsible for inland flooding associated with TC Camille (1969) and the inland reintensification of TC Danny (1997). The interaction of each storm with an equatorward entrance region of an upper-tropospheric jet links the two cases; however, TC Camille did not undergo inland reintensification. TC Camille will serve as a null case of an inland reintensifying TC in an equatorward entrance region of an upper-tropospheric jet to identify synoptic-scale influences that limit a TC from undergoing inland reintensification. For historical context, the TC Danny inland reintensification case will be compared with other cases of inland reintensifying TCs east of the Rocky Mountains from 1950 through 2010. Similarities and differences between TC Camille and TC Danny will be discussed toward the end of this thesis, which will be beneficial in understanding the specific conditions needed to bring about various inland TC impacts. These similarities and differences will provide forecasters information they can utilize to predict the threats associated with inland TC–midlatitude jet interactions. To provide further background on this research topic, the rest of this chapter will discuss previous research documenting the various interactions that take place between TCs and the midlatitude flow. Topics from the previous research will include interactions during extratropical transition (ET), TC intensification, and interactions associated with inland flooding.

1.2 Motivation and Overview

A growing awareness of societal impacts associated with landfalling and transitioning TCs in recent decades has led to increasing attention to the interactions between TCs and the midlatitude flow. Although our understanding of these interactions has improved, research is needed to provide additional insight into localized effects of inland-moving TCs. Accurate numerical forecasts continue to be a problem because of the relatively small scale of TCs and the complex physical processes that occur during the interactions between a TC and the midlatitude environment (Jones et al. 2003). Forecast challenges include cases which undergo strong ET in the midlatitudes, result in reintensification prior to landfall or over the ocean where shipping lanes are impacted, and produce severe inland flooding. According to Rappaport (2000), in a 30-yr (1970–1999) study of fatality statistics associated with TCs and their remnants, more than half of the 600 U.S. deaths were caused by freshwater flooding. Most of these freshwater fatalities were located inland.

One of the most severe cases of inland flooding can be attributed to TC Camille, which has not been given as much retrospective scrutiny as TC Connie (1955; Dunn et al. 1955; Namias and Dunn 1955), TC Diane (1955; Dunn et al. 1955; Namias and Dunn 1955), TC Agnes (1972; Carr and Bosart 1978; Bosart and Dean 1991), TC Fran (1996; Pasch and Avila 1999), and TC Floyd (1999; Atallah and Bosart 2003; Colle 2003). TC Camille is unique since the severe localized flooding observed in the mountains of west-central Virginia occurred while TC Camille was weakly transitioning into an extratropical cyclone as identified by Chien and Smith (1977). Therefore, an examination

of this event would be beneficial to understanding the specific setup needed to produce severe inland flooding.

When a TC moves over land, the surface sensible and latent heat fluxes are greatly reduced, which weakens the TC. In special circumstances, a TC can reintensify while over land: TC David (1979; Bosart and Lackmann 1995), TC Danny (1997; Bassill and Morgan 2006), and TC Erin (2007; Arndt et al. 2009; Monteverdi and Edwards 2010; Evans et al. 2011). The lack of documentation of inland reintensifying TCs provides an opportunity to better understand the mechanisms and processes that lead to such an event, which gives motivation for analyzing the TC Danny case more in depth. Whereas Bassill and Morgan (2006) provided a first-look analysis of the inland reintensification of TC Danny, a more complete and detailed analysis will be conducted in this thesis.

1.3 Interactions between TCs and Midlatitude Troughs and Jets

1.3.1 ET of TCs

As a TC moves from the tropics into the midlatitudes, it may interact with the midlatitude flow and undergo ET. The ET process was split into two stages by Klein et al. (2000): 1) the transformation and 2) the reintensification stages. The transformation stage of ET has been well documented (e.g., DiMego and Bosart 1982a,b; Sinclair 1993; Harr and Elsberry 2000; Klein et al. 2000; Atallah and Bosart 2003; Jones et al. 2003) and is described by Klein et al. (2000) as the process where the TC circulation becomes tilted and transforms from a barotropic to a baroclinic system (Fig. 1.1). In this process, a lower-tropospheric temperature advection dipole develops, where cold, dry air wraps into the TC circulation from the west, and warm, moist air moves poleward east of the

circulation and ascends over tilted isentropic surfaces associated with a preexisting baroclinic zone. In the latter region, typically northeast of the TC circulation, there is enhanced precipitation. Although the process of ET is well understood, defining the exact onset of ET is still problematic. Recent studies have suggested that the onset of ET may occur when the rate of increase in frontogenesis peaks (Harr et al. 2000) or can be detected by using a phase diagram of thermal wind and thermal asymmetry (Hart 2003).

After the transformation stage is complete, intensification of the prior TC as an extratropical cyclone may take place. Most studies have acknowledged that the structure of the midlatitude circulation affects whether an extratropical cyclone will intensify or weaken (e.g., Harr et al. 2000; Klein et al. 2002; Sinclair 2002; Ritchie and Elsberry 2003; Sinclair 2004; Hart et al. 2006; Ritchie and Elsberry 2007). In the North Pacific, Harr et al. (2000) found that a northwest (northeast) pattern is typically associated with ET in that region. A northwest pattern is characterized by a midlatitude trough that is located northwest of a poleward-moving TC, whereas a northeast pattern is characterized by a large quasi-stationary midlatitude cyclone that is located northeast of a poleward-moving TC. Harr et al. (2000) found that a northwest (northeast) pattern is typically associated with a strengthening (weakening) extratropical cyclone after ET (Fig. 1.2). Harr et al. (2000) diagnosed the differences between the two patterns by evaluating low-level eddy heat fluxes and an energy budget. Simulations conducted by Ritchie and Elsberry (2003) found that the strength of a midlatitude trough had no impact on the final intensification of a transitioned TC after ET. Expanding upon the research conducted by Ritchie and Elsberry (2003), Ritchie and Elsberry (2007) investigated whether the phasing between a remnant TC and an upper-tropospheric trough had an impact on the

final intensification of the transitioned TC after ET. Ritchie and Elsberry (2007) showed that the phasing of the remnant TC with an upstream midlatitude trough was important for enabling extratropical cyclogenesis.

In addition to a midlatitude trough, the interaction of a transitioning TC with a midlatitude upper-tropospheric jet has been documented. The diabatically driven outflow associated with a TC has been shown to impact the magnitude of an upper-tropospheric midlatitude jet and downstream geopotential height field (e.g., Archambault 2011; Fig. 1.3). In a climatology of recurving Northwest Pacific TCs, Archambault (2011, chapter 2) explains that the upper-tropospheric irrotational wind, indicative of the diabatically driven outflow, is directed radially outward from the ascent region associated with a recurving TC and into the meridional potential vorticity (PV) gradient. Lower values of PV are advected by the upper-tropospheric irrotational wind towards higher values of PV, which tightens the meridional PV gradient. As a result, jet streak intensification and upper-tropospheric ridge amplification may occur. The locations of these recurving TCs were generally found to be in the equatorward entrance region of an upper-tropospheric jet, which corresponds to a region of upper-level divergence and, therefore, with tropospheric-deep ascent (Uccellini and Kocin 1987; Fig. 1.4). The jet-entrance region is typically associated with a thermally direct secondary circulation, where divergent (convergent) ageostrophic winds are found on the equatorward (poleward) side of the jet-entrance region.

1.3.2 Intensification Changes of TCs

A TC may intensify when the system is in a favorable environment (e.g., low vertical wind shear, warm sea surface temperatures, moist conditions in the lower-to-middle troposphere). However, studies have shown that TCs can intensify when interacting with midlatitude troughs and jets, which are associated with higher wind shear than observed during TC development (e.g., Molinari and Vollaro 1989; Molinari and Vollaro 1990; Shi et al. 1990; Molinari et al. 1995; Shi et al. 1997; Molinari et al. 1998; Bosart et al. 2000; Hanley et al. 2001; Hanley 2002; Kimball and Evans 2002; Yu and Kwon 2005; Rappin et al. 2011). Among these cited studies, the interactions between TCs and troughs have been analyzed using diagnostics [eddy flux convergence (EFC; e.g., Molinari and Vollaro 1989; Yu and Kwon 2005); Ertel PV (e.g., Molinari et al. 1995; Hanley et al. 2001)], observations [satellite imagery (e.g., Bosart et al. 2000; Hanley 2002)], and three-dimensional models (e.g., Kimball and Evans 2002; Rappin et al. 2011).

Molinari and Vollaro (1989) used calculations of EFC to diagnose the rapid intensification of Hurricane Elena (1985) over the Gulf of Mexico. When analyzing the calculated values of EFC, Molinari and Vollaro (1989) found a high correlation between the angular momentum fluxes by azimuthal eddies at large radii and central pressure changes in the storm 27–33 h later (Fig 1.5). Molinari and Vollaro (1989) also noted an inward shift of cyclonic eddy momentum that was produced by the passage of a midlatitude trough poleward of Hurricane Elena. Sources of anticyclonic eddy momentum removal from the TC circulation included the west-southwesterly flow ahead of the trough and the outflow jet equatorward of the TC. A subsequent study by Molinari

and Vollaro (1990) would argue the trough was not a direct cause of the deepening, but a catalyst that produced locally enhanced surface fluxes and associated convection that supported the formation of a contracting secondary eyewall.

Upper-tropospheric jets have also been documented to impact TC intensification. Simulations of a TC–jet interaction conducted by Rappin et al. (2011) show that the convective outflow associated with a TC modifies an upper-tropospheric jet, resulting in a weaker shear environment and rapid intensification of the TC–jet couplet. Shi et al. (1997) observed a high correlation between an approaching upper-tropospheric jet with a sudden burst of inner-core convection associated with Hurricane Florence (1988). The increased convection was said to be crucial to the intensification of Hurricane Florence, which is similar to the argument made by Bosart et al. (2000) documenting the rapid intensification of Hurricane Opal (1995).

In the 12-yr period from 1985 through 1996, Hanley et al. (2001) used values of EFC greater than 10 (m s^{-1}) day^{-1} to identify TC–trough interactions. A total of 146 interactions were identified and sorted into four distinct composites of TC–trough interactions: favorable distant interaction, favorable superposition, unfavorable distant interaction, and unfavorable superposition. Distant interactions were identified when an upper-tropospheric PV maximum was between 1000 km and 400 km from the TC center, while a superposition was deemed to take place when a PV maximum was within 400 km of the TC center. A composite of the favorable distant interactions shows a PV trough well to the west of and comparable in size to the TC (Fig. 1.6). The TC is located underneath the entrance region of an upper-tropospheric jet, where upper-level divergence is occurring. The comparable size of the PV trough to the size of the TC was

believed to be important in enabling a favorable interaction between the two features. The effect of reduced vertical wind shear over the TC circulation was thought to be the main reason for the favorable interaction. Similar arguments concerning the comparable trough to TC size have been made in previous studies (Molinari et al. 1995; Bosart et al. 2000).

1.3.3 Inland Flooding Associated with TCs

As previously mentioned, flooding associated with TCs is the largest contributor to TC-related fatalities, which are mainly located inland (Rappaport 2000). A 49-yr (1950–1998) climatology of precipitation distributions associated with landfalling TCs was conducted by Atallah et al. (2007). Their climatology was split into left-of-center (LOC) and right-of-center (ROC) composites showing the environmental setup favoring each distribution pattern (Fig. 1.7). LOC precipitation distributions are identified to have an upper-tropospheric trough upstream of the TC circulation, with positive (negative) PV advection tendencies southwest (northeast) of the TC. ROC precipitation distributions are associated with a TC embedded upstream of an upper-tropospheric ridge axis and downstream of a weak and shallow upper-tropospheric trough. Only a negative PV advection tendency is seen to the northeast of the TC, resulting from latent heat release associated with precipitation.

Heavy precipitation associated with TCs has been documented to occur in the presence of surface frontogenesis (e.g., Bosart and Dean 1991), upper-level divergence associated with an upper-tropospheric jet (e.g., DeLuca 2004), and cold-air damming (e.g., Srock and Bosart 2009). Mesoscale distributions of heavy rainfall associated with TCs over the Northeast U.S. were documented by Klein (2007). In similar fashion to

Atallah et al. (2007), Klein (2007) broke down precipitation distributions into left-of-track (LOT) and right-of-track (ROT) distributions. The LOT distributions were associated with an upper-tropospheric jet poleward of the TC center, whereas ROT distributions had an upper-tropospheric jet farther downstream and to the northeast of the TC. Klein (2007) noted that the heaviest rainfall occurs along and on the cold side of mesoscale surface boundaries in both LOT and ROT distributions. Vertical cross sections of frontogenesis and upward vertical motion for LOT and ROT distributions are shown in Fig. 1.8. For LOT distributions, tropospheric-deep frontogenesis and the ascent pattern tilts towards the cold air with increasing height with ascent maximized in the midtroposphere on the warm side of the frontogenesis maximum. For ROT distributions, surface frontogenesis is dominant and the ascent pattern is upright and located on the warm side of the frontogenesis maximum with ascent maximized above the boundary layer. For both LOT and ROT distributions, the presence of a cyclonically curved lower-tropospheric jet to the east side of the TC enhances the poleward flux of tropical air from the Atlantic into the surface frontal boundary.

In the past five years, research has gone into understanding a newly identified contributor to inland flooding associated with TCs. The term “predecessor rain event (PRE)” was first coined by Cote (2007), where he documented the spatial structure and temporal evolution of a mesoscale region of heavy rainfall separate from the main TC rain shield that develops poleward of landfalling or coastal-tracking Atlantic basin TCs. Based on his 9-yr climatology, from 1998 through 2006, Cote (2007) noted that PREs are associated with the transport of anomalously high moisture directed towards a lower-tropospheric baroclinic zone underneath an equatorward entrance region an upper-

tropospheric jet. Most PREs were located approximately 1000 km poleward of the TC and occurred 36 h before the arrival of the TC. After Cote (2007), several studies have verified the findings of his research and have provided more case-specific analyses of PREs (e.g., Galarneau et al. 2010; Moore 2010; Schumacher et al. 2011; Bosart et al. 2012). In an extended climatology (1988–2008), Moore (2010) stratified PREs into three categories based upon the upper-tropospheric setup within which the PRE and TC were embedded: jet in ridge (JR), southwesterly jet (SJ), and downstream confluence (DC) (Fig. 1.9). An overriding characteristic of each conceptual model is the presence of a moist, lower-tropospheric jet east of the TC that is directed towards a lower-tropospheric baroclinic zone underneath an equatorward entrance region of an upper-tropospheric jet.

1.4 Documented Cases of Inland Reintensifying TCs

As previously stated, there have been only three documented cases of an inland reintensifying TC: TC David (1979; Bosart and Lackmann 1995), TC Danny (1997; Bassill and Morgan 2006), and TC Erin (2007; Arndt et al. 2009; Monteverdi and Edwards 2010; Evans et al. 2011). Although each case reintensified while over land, the mechanisms and processes that led to the strengthening of each TC differ.

The reintensification of TC David occurred over the Northeast U.S. about 36 h after making a final landfall over southeast Georgia. As TC David traversed poleward across Pennsylvania, it reintensified in response to tropopause lifting ahead of a weak upper-tropospheric trough due to diabatic heating from deep convection associated with the TC (Bosart and Lackmann 1995). Reduction of the upper-tropospheric trough wavelength occurred in conjunction with diabatically driven down-shear ridge building,

which led to increased cyclonic vorticity advection over TC David as this trough approached from the southwest. The associated ascent and low-level horizontal convergence created a favorable environment for generating cyclonic vorticity within the moist neutral thermodynamic environment around TC David. The development of an upper-tropospheric jet poleward of TC David also aided in the ascent around the TC circulation.

The inland reintensification of TC Danny over the Carolinas occurred approximately four days after making a final landfall in southern Alabama. Cyclonic vorticity advection from an approaching upstream trough, upper-level divergence situated in the equatorward entrance region of an upper-tropospheric jet, and vortex tube stretching as the storm traversed the southern Appalachian Mountains were the main reasons for the inland reintensification of TC Danny (Bassill and Morgan 2006). All of these factors, in addition to the moist neutral thermodynamic environment surrounding TC Danny, were important in the generation of near-surface cyclonic vorticity. Bassill and Morgan (2006) found that low values of PV generated above and poleward of TC Danny was associated with latent heat release in the presence of deep convection. The generation of low values of PV ahead of the upstream trough, characterized by higher values of PV, tightened the meridional PV gradient and led to an intensification of the upper-tropospheric jet poleward of TC Danny. The low values of PV also served to decrease the vertical wind shear above the TC, which was conducive for intensification.

The reintensification of TC Erin over Oklahoma is unique because of its location over the southern Plains and the dense observational network provided by the Oklahoma Mesonet during the event (Arndt et al. 2009). In addition, TC Erin did not have the

upper-level support seen in the TC David and TC Danny cases. However, the moist neutral thermodynamic environment surrounding TC Erin favored low-level convergence, deep rising motion, and near-surface cyclonic vertical vorticity generation (Evans et al. 2011). A southerly lower-tropospheric jet extending from the Gulf of Mexico provided moisture and generated instability in the region ahead of TC Erin. Evans et al. (2011) further showed that anomalously wet months (March through July 2007) preceding TC Erin had the greatest positive impact on its reintensification among three analyzed soil moisture-related signals: a seasonal signal, an along-track rainfall signal, and an early postlandfall rainfall signal. The high soil moisture content resulting from the anomalously wet months provided moisture and greater instability in the boundary layer. Inland TC reintensification has been found to occur in situations where the underlying surface has high heat conductivity and is relatively moist (Shen et al. 2002), and when rainfall ahead of a TC falls on desert soils and provides sufficient surface heat fluxes for a TC to reintensify (Emanuel et al. 2008).

1.5 Goals and Organization of Thesis

The main goals of this thesis are to: (1) document the synoptic-scale environment and underlying mesoscale processes responsible for inland flooding associated with TC Camille (1969) and the inland reintensification of TC Danny (1997); (2) explain similarities and differences between the TC Camille and TC Danny cases; and (3) document important mechanisms and processes that lead to various impacts associated with inland TC–midlatitude jet interactions.

The remainder of this thesis will be organized as follows. Chapter 2 will discuss the data and methods used to construct the list of inland reintensifying TCs and to conduct the two multiscale analyses. The multiscale analyses of TC Camille and TC Danny will be documented in Chapter 3 and Chapter 4, respectively. Chapter 5 will compare and contrast the two TC cases, and provide concluding remarks and suggestions for future work.

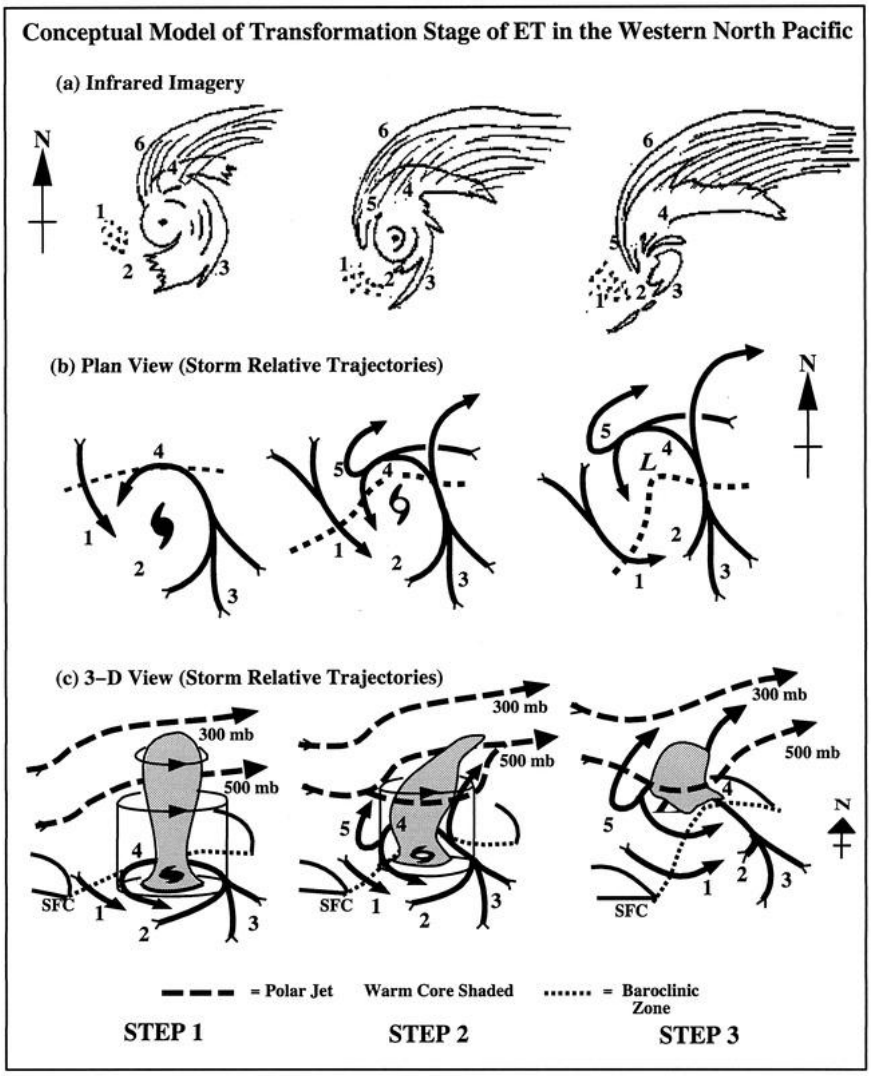

Fig. 1.1. Conceptual model of transformation stage of ET in the western North Pacific, with labeled areas as follows: 1) environmental equatorward flow of cooler, drier air (with corresponding open cell cumulus); 2) decreased TC convection in the western quadrant (with corresponding dry slot) in step 1, which extends throughout the southern quadrant in steps 2 and 3; 3) environmental poleward flow of warm, moist air is ingested into TC circulation, which maintains convection in the eastern quadrant and results in an asymmetric distribution of clouds and precipitation in steps 1 and 2; steps 2 and 3 also feature a southerly jet that ascends tilted isentropic surfaces; 4) ascent of warm, moist inflow over tilted isentropic surfaces associated with baroclinic zone (dashed line) in middle and lower panels; 5) ascent (undercut by dry-adiabatic descent) that produces cloudbands wrapping westward and equatorward around the storm center; dry-adiabatic descent occurs close enough to the circulation center to produce erosion of eyewall convection in step 3; 6) cirrus shield with a sharp cloud edge if confluent with polar jet. Caption and figure reproduced from Fig. 5 in Klein et al. (2000).

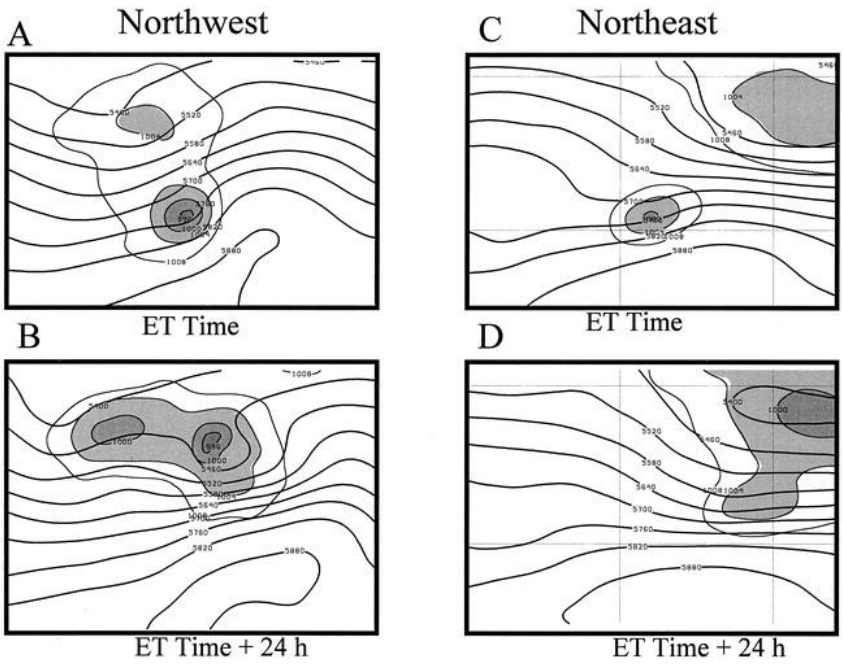

Fig. 1.2. Composite 500-hPa height (m) and sea level pressure (hPa, only below 1008 hPa with shading in 4-hPa increments starting at 1004 hPa) analyses based on grouping of cases in a northwest pattern at the (a) ET time, (b) ET + 24 h, and in a northeast pattern at the (c) ET time and (d) ET + 24 h. The composite northwest pattern is based on 13 cases and the northeast pattern is based in 17 cases. Caption and figure reproduced from Fig. 1 in Harr et al. (2000).

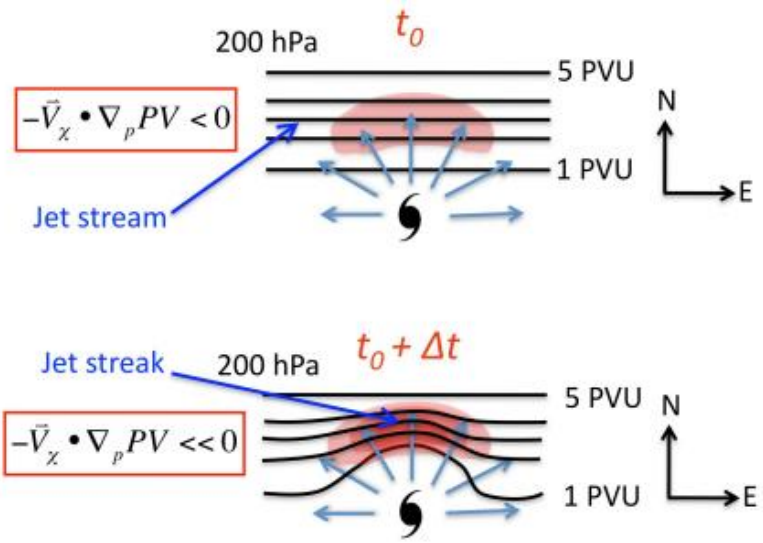

Fig. 1.3. Schematic representation of upper-tropospheric ridge amplification and jet streak intensification associated with divergent TC outflow impinging upon an upper-tropospheric jet stream (i.e., a meridional PV gradient). Caption and figure reproduced from Fig. 2.6 in Archambault (2011).

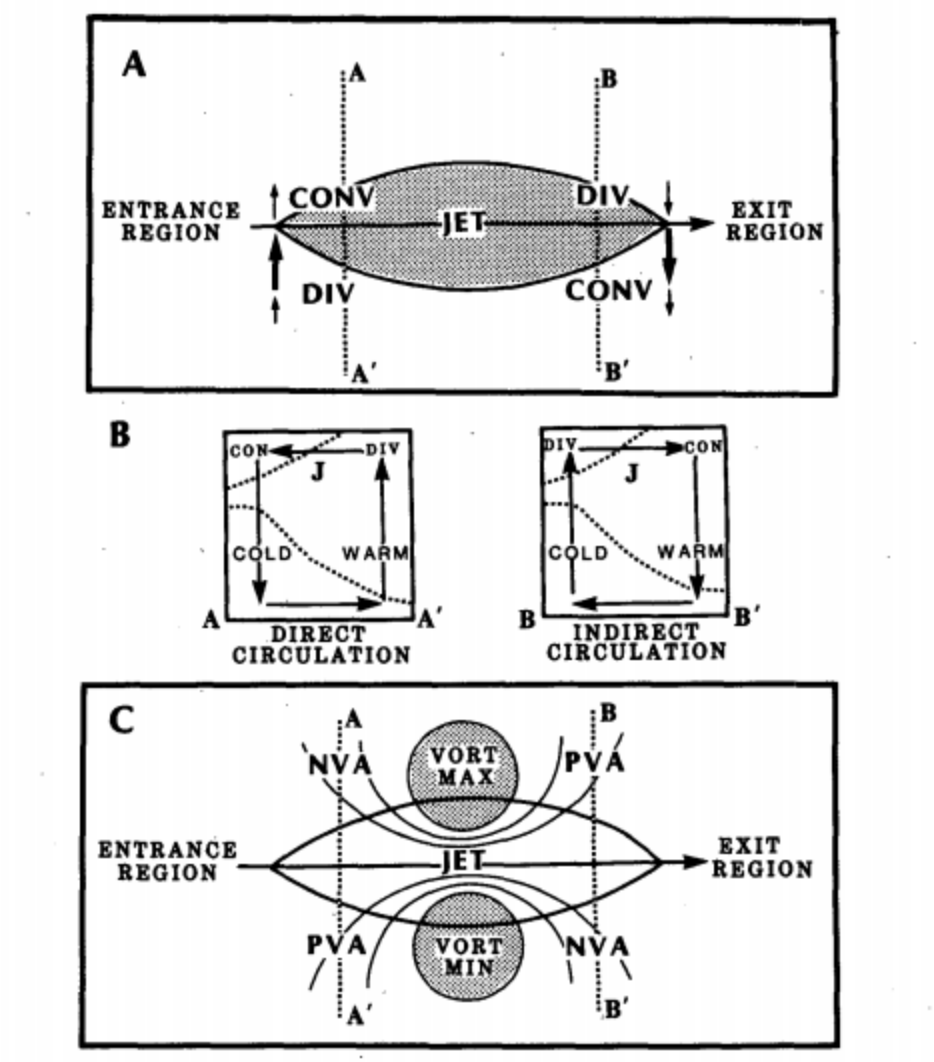

Fig. 1.4. (a) Schematic of transverse ageostrophic wind components and patterns of divergence associated with the entrance and exit regions of a straight jet streak [after Bjerknes (1951)]. (b) Vertical cross sections illustrating direct and indirect circulations in the entrance region [along dotted line labeled A–A′ in (a)] and exit region [along dotted line labeled B–B′ in (a)] of a jet streak. Cross sections include two representative isentropes (dotted), upper-tropospheric jet location (marked by a J), relative positions of cold and warm air, upper-level divergence, horizontal ageostrophic components, and vertical motion (arrows) within the plane of each cross section. (c) Schematic of maximum (cyclonic) and minimum (anticyclone) relative vorticity centers and associated advection patterns associated with a straight jet streak. (NVA represents negative or anticyclonic vorticity advection; PVA represents positive or cyclonic vorticity advection.) Caption and figure reproduced from Fig. 3 in Uccellini and Kocin (1987).

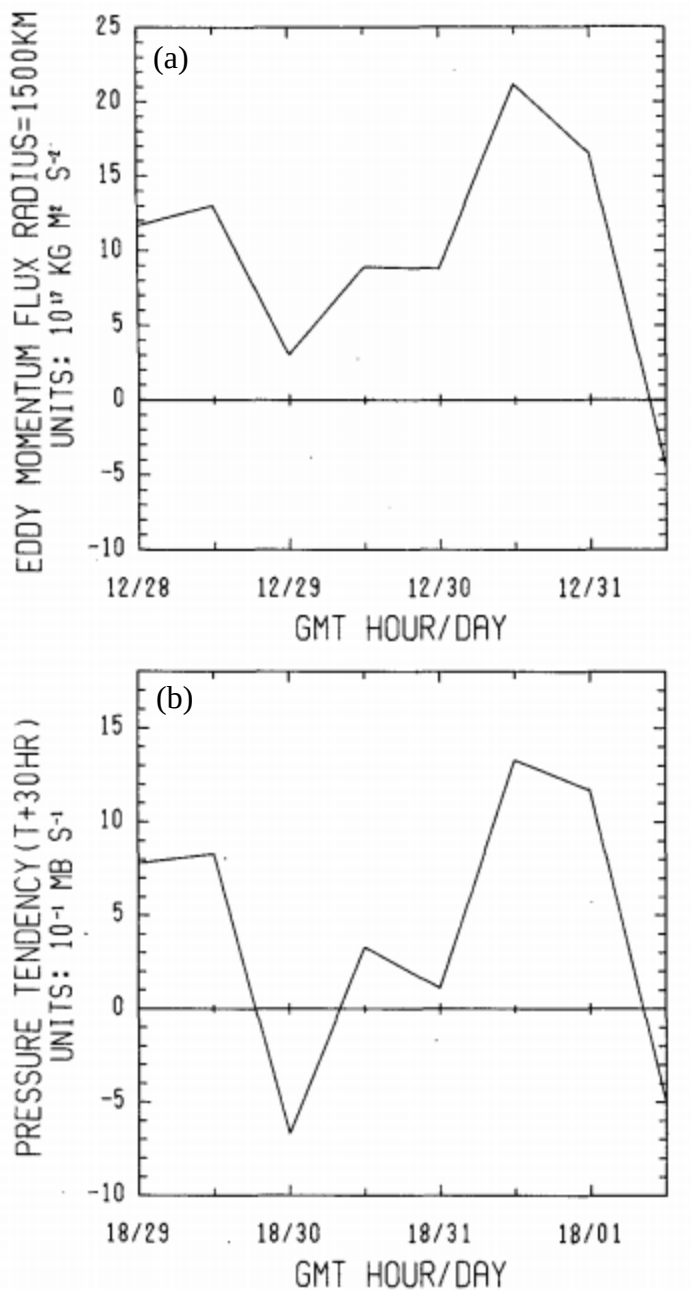

Fig. 1.5. (a) Eddy momentum flux at the 1500 km radius, plotted only for those times in which the storm remained over water 30 h later. (b) Deepening rate of the storm at times 30 h after those of part (a). Caption and figure reproduced from Fig. 4 in Molinari and Vollaro (1989).

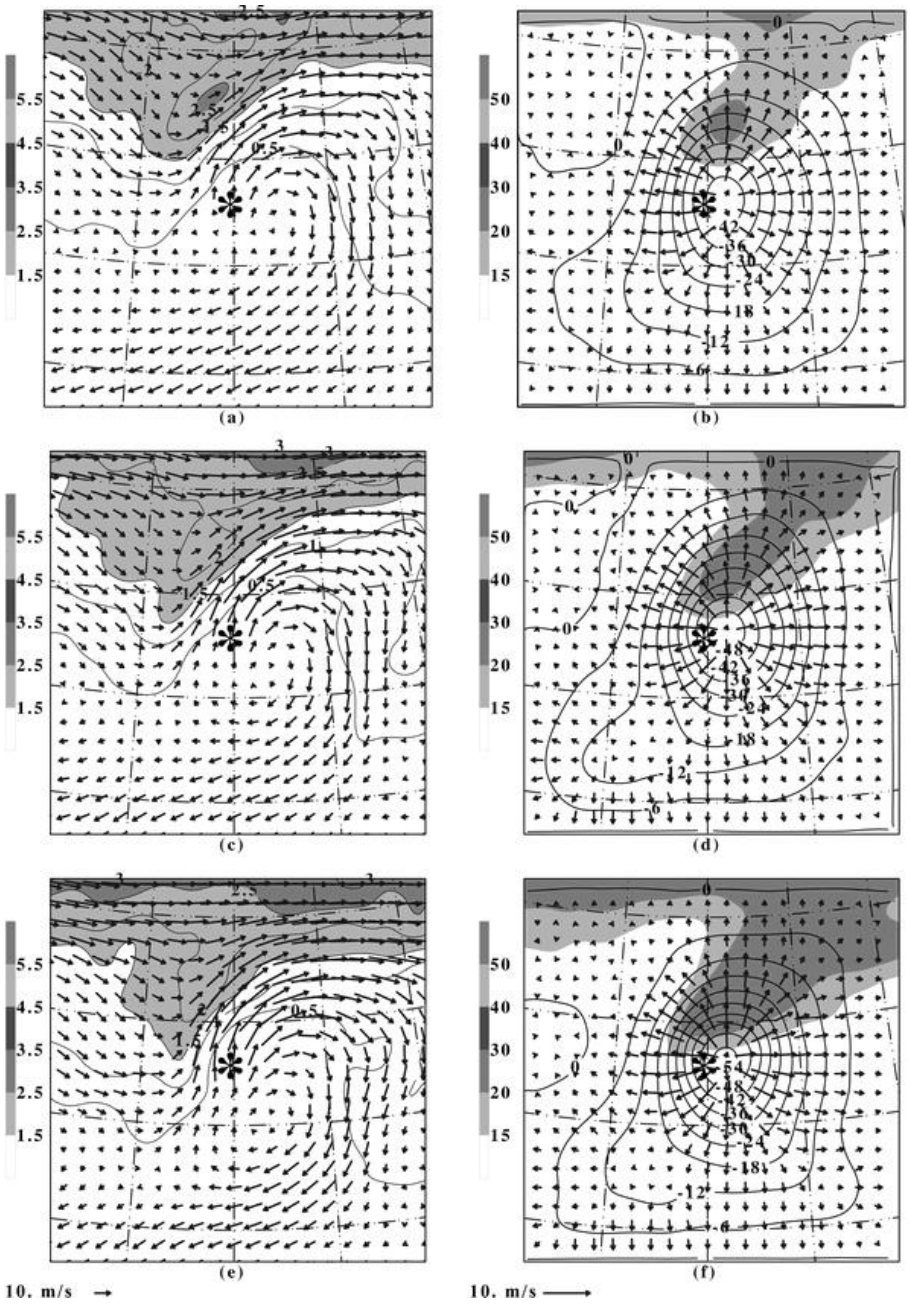

Fig. 1.6. Horizontal plot on the 200-hPa surface for the favorable distant interaction composite containing cases with a total δp of more than 10 hPa. (a), (c), and (e) Vectors of the total wind [m s^{-1}, reference arrow indicated at bottom left of (e)] and Ertel PV (increment is 0.5 PVU and values greater than 1.5 PVU are shaded as indicated) at times $t_0 - 12$ h, t_0, and $t_0 + 12$ h, respectively. (b), (d), and (f) Total wind speed (m s^{-1}, values greater than 15 m s^{-1} are shaded as indicated), velocity potential φ (solid lines, contour interval 6×10^5 m^2 s^{-1}), and divergent wind $\mathbf{V}_d$ [m s^{-1}, reference arrow indicated at bottom left of (f)] at times $t_0 - 12$ h, t_0, and $t_0 + 12$ h, respectively. Asterisk denotes the location of the composite TC center, and the increment in latitude and longitude is 10°. Caption and figure reproduced from Fig. 5 in Hanley et al. (2001).

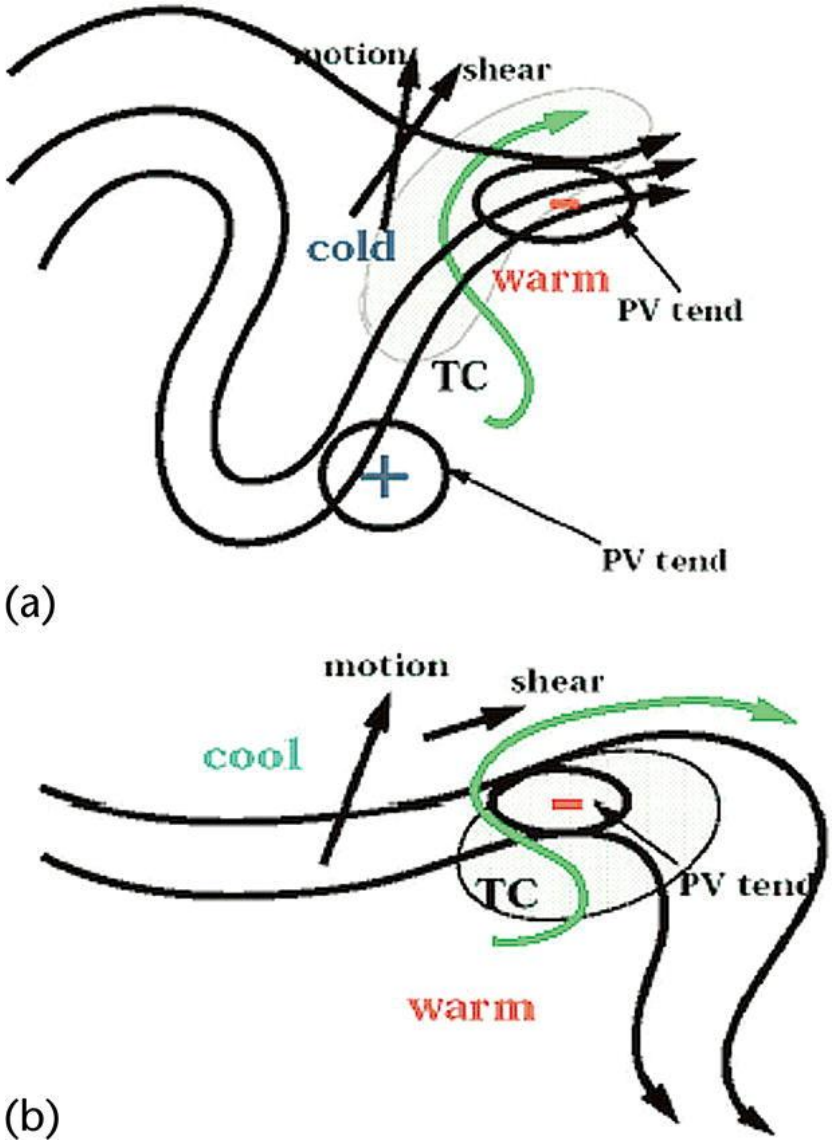

Fig. 1.7. Schematics for landfalling TCs for (a) the LOC composite and (b) the ROC composite. The curved black lines represent streamlines of the upper-tropospheric (i.e., 250 hPa) flow. Arrows represent motion and deep tropospheric shear with the relative magnitudes given by the length of the arrow. The curved green line represents the trajectory of a parcel starting near the surface in the warm sector and ending in the mid- to upper troposphere in the cool sector. The gray shaded area represents regions of precipitation and pluses and minuses represent the local PV tendency resulting from a combination of advection and the diabatic redistribution of PV. Caption and figure reproduced from Fig. 10 in Atallah et al. (2007).

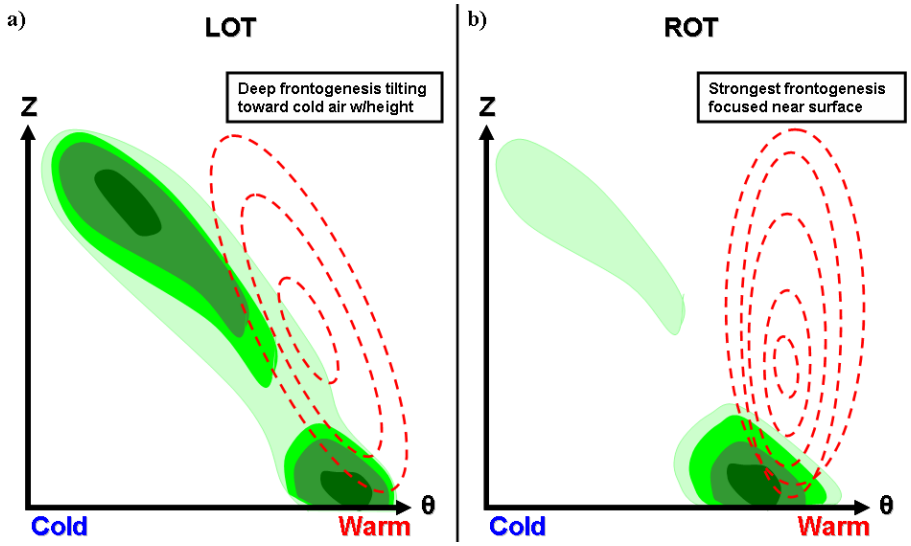

Fig. 1.8. Schematic cross section of the warm-frontal boundary found in (a) LOT precipitation distribution cases and (b) ROT precipitation distribution cases. Cross section includes frontogenesis shaded in green and vertical velocity dashed contoured in red. Caption and figure reproduced from Fig. 4.3 in Klein (2007).

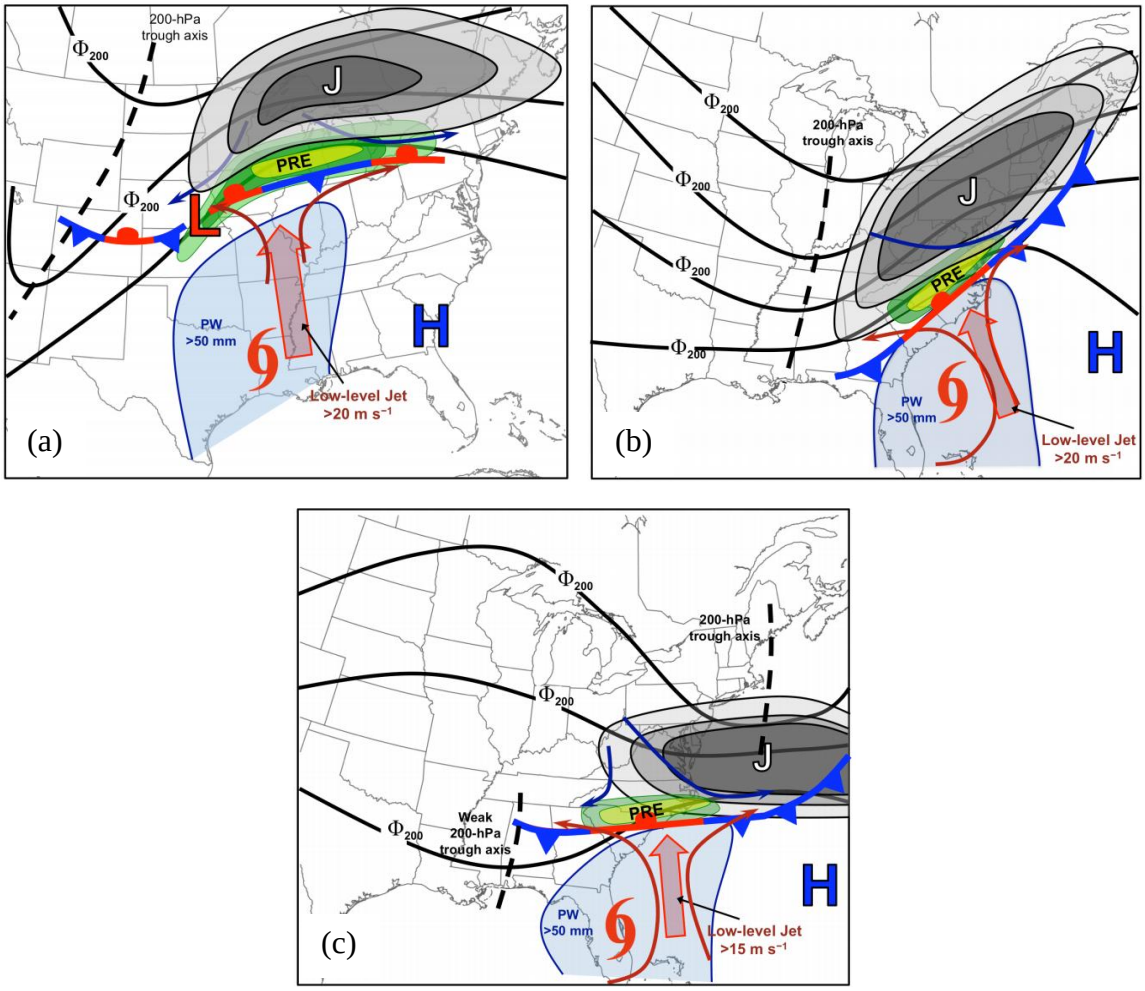

Fig. 1.9. Conceptual model of the synoptic-scale environment of (a) JR, (b) SJ, and (c) DC category PREs showing 200-hPa geopotential height (solid black contours), 200-hPa wind speed (gray shading; "J" symbol marks the location of maximum wind speed), low-level (i.e., 925-hPa) streamlines (red indicates warm advection, blue indicates cold advection), the lower-tropospheric jet (large red arrow), the lower-tropospheric baroclinic zone (stationary front symbol), and precipitable water (PW; values > 50 mm shaded in blue). The position of the PRE is indicated by the green shading, the position of the TC is indicated by the tropical storm symbol, and the maxima and minima in low-level geopotential height are indicated by the "H" and "L" symbols, respectively. Caption and figures reproduced from Figs. 6.1, 6.2, and 6.3 in Moore (2010).